Materials challenges for next-generation high-density magnetic recording: media and read heads

K. Hono
Magnetic Materials Unit
National Institute for Materials Science

Collaborators
T. Furubayashi, Y. Sakuraba, Y. K. Takahashi
S. T. Li, J. Chen, Du Ye, T. T. Sasaki

National Institute for Materials Science (NIMS)

http://www.nims.go.jp/apfim/

National Institute for Materials Science
Established in April 2001
World's Core Institute in Materials Research –

- Advanced Key Technologies Division
- Nanoscale Materials Division (MANA)
- Energy & Environment Materials Division

450 staff scientists
~$200 million

Magnetic Materials Unit - NIMS

Magnetic and spintronics materials for data storage and energy saving by nanostructure control

magnetic recording

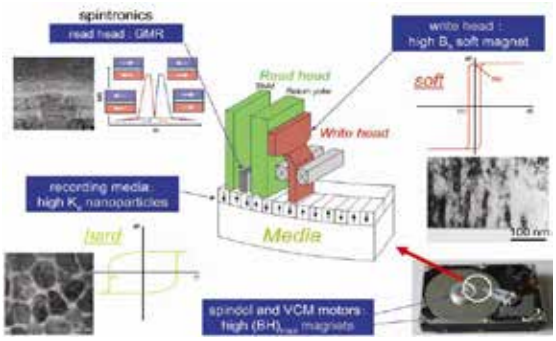

permanent magnets

hybrid vehicles
electric vehicles

nanostructure analysis

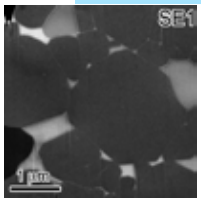

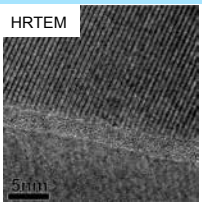

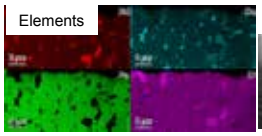

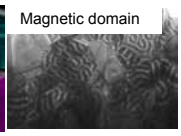

Atom probe tomography

spintronics devices

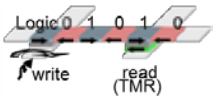

Magnetic Domain Wall Memory and Logic

STT-MRAM

Magnetic Materials Unit - NIMS

Magnetric Materials Group

Development of magnetic materials for magnetic recording and spintronics

K. Hono T. Furubayashi Y. K. Takahashi Y. Sakuraba

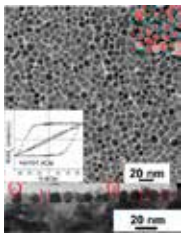

high K_u films

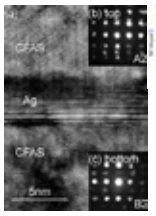

CPP-GMR

High spin-polarization materials

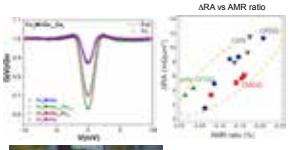

Nanoanalysis Group

C_s-corrected STEM

T. Ohkubo T. T. Sasaki H. Sepehri-Amin

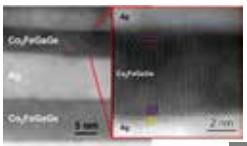

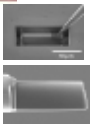

Laser assisted 3DAP

Structure-property correlations of magnetic and spintronic devices

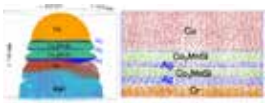

Spintronics Group

S. Mitani S. Kasai M. Hayashi H. Sukegawa

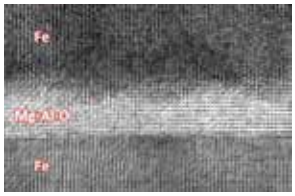

Low RA, high MR p-MTJ using new materials

High density magnetic recording > 2 Tbit/in^2

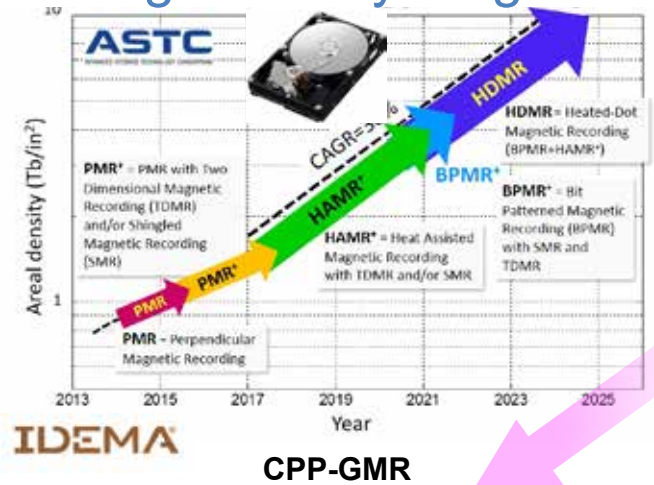

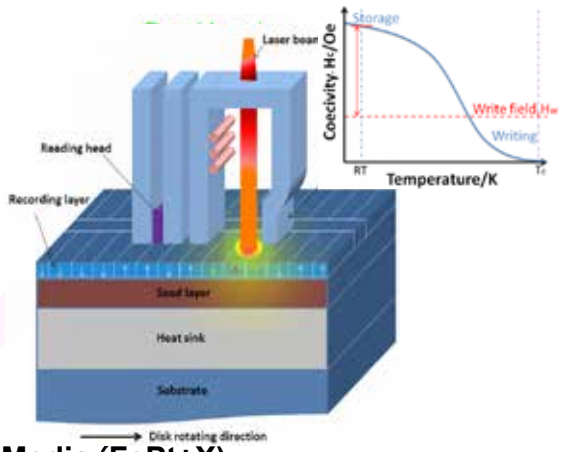

CPP-GMR

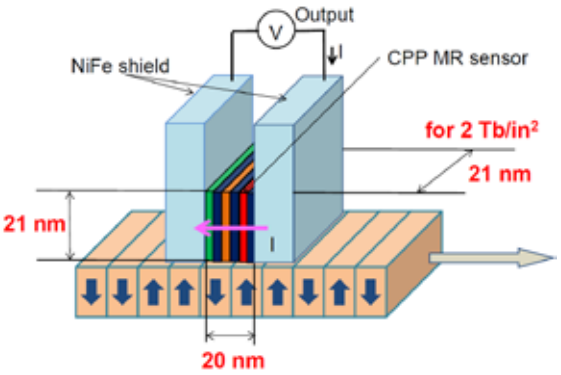

Media (FePt+X)

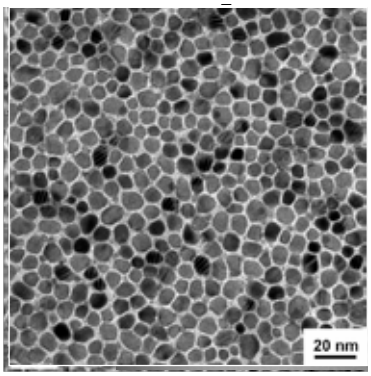

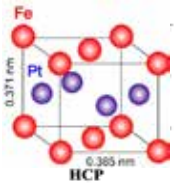

K_u=7 MJ/m^3
D_p~2.5 nm

FePtAg-C prototype MAMR media

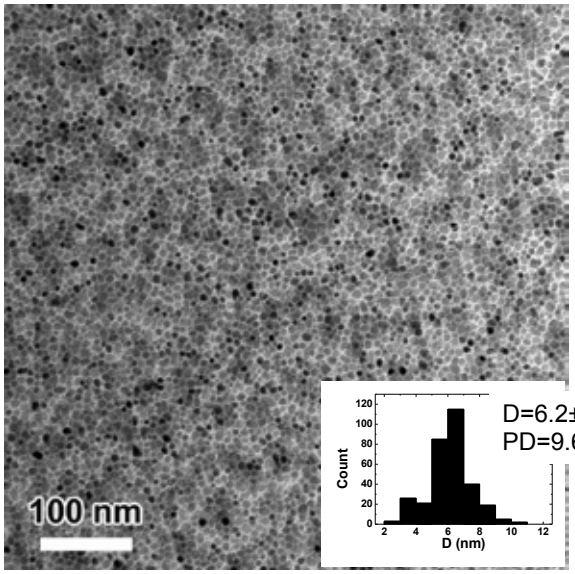

D=6.2±1.4 nm
PD=9.6 nm

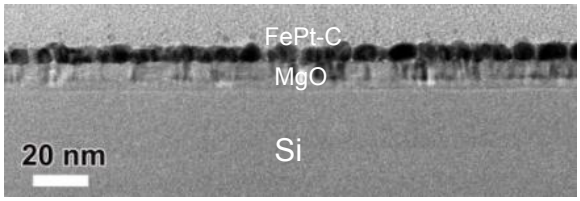

t=6.4 nm

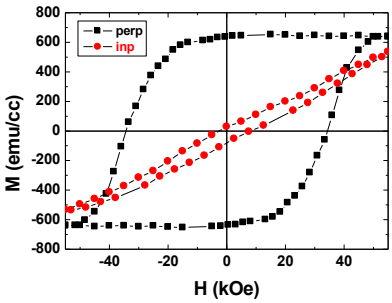

H_C= 35 kOe
K_u = 4.3 MJ/m^3
ΔH_C = 6 kOe

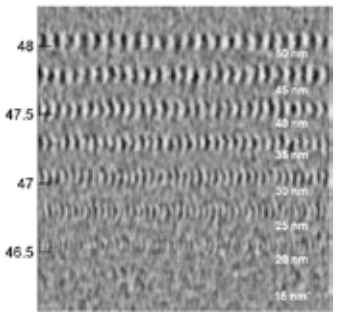

Track width 92nm
Min. bit length 15nm
Areal density ~ 550Gbits/in^2
(TAR static test HGST)

L. Zhang, Y. K. Takahashi, K. Hono, B. C. Stipe, J.-Y. Juang, and M. Grobis, IEEE Trans. Magn. 47, 4062 (2011).

$L1_0$-FePt HAMR media for 2 Tbps

Areal Density (Tbit/in^2)	2	4
Grain size, D (nm)	6	4.3
Pitch distance, D_p (nm)	7	5.1
Size distribution, s (%)	10 – 15	10 – 15
$\mu_0 M_s$ of FM layer (T)	0.88	1
$\mu_0 M_s$ of FM grain (T)	1.1	1.26
K_u (MJ/m^3)	3.5	5
$\mu_0 H_k$ (T)	8	10
s_{Hk}/H_k	5 – 10	5 -10
T_c (°C)	480	430
s_{Tc}/Tc (%)	2	2
EA distribution, s_α (°)	2	0.8
Media thickness, t (nm)	9	8.2
Grain aspect ratio (h/D)	1.29	1.6
Number of grains/bit	6.7	6.2

D. Weller et al. IEEE Trans. Magn. **50**, 3100108 (2014).

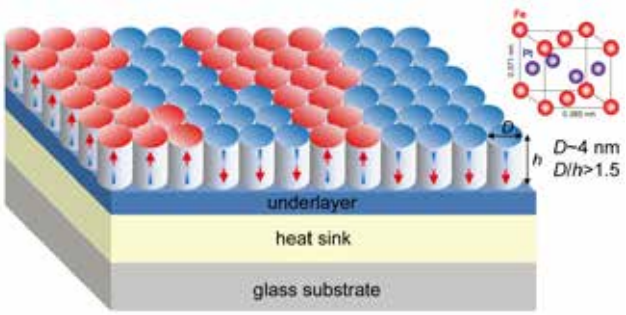

FePt-X granular media for >2 Tbit/in^2

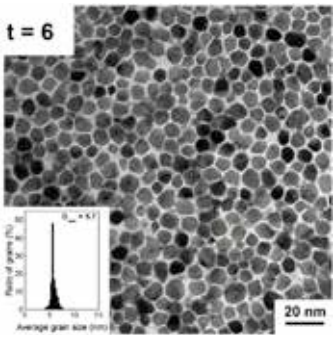

D ~ 6 nm
PD ~ 7 nm
σ<10-15%
h/D ~ 1.3
t > 9 nm
EA distribution < 2°
R_a<0.04 nm

How to grow columnar grains in the FePt-C system?

compositionally graded sputtering process

Co-sputter

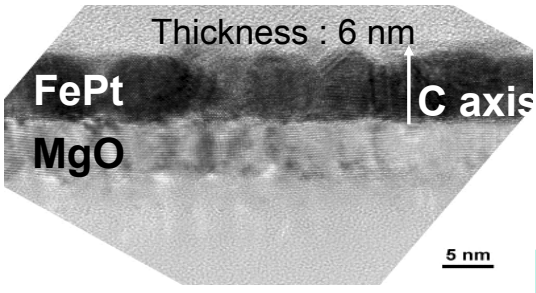

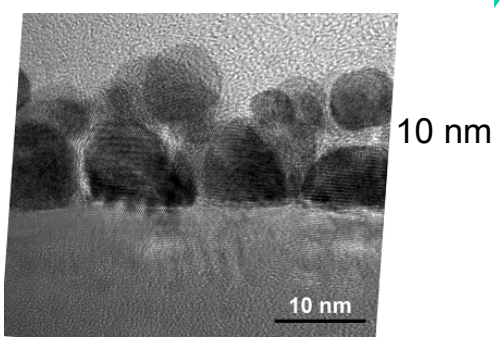

Cosputter of Fe, Pt and C

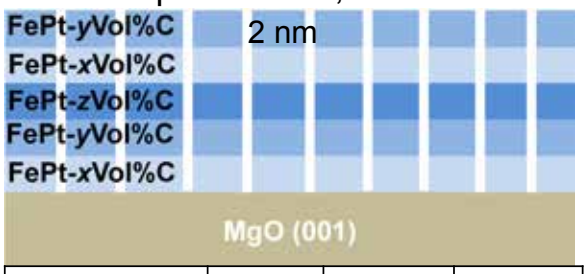

	x	y	z
FePt-20%C	15	20	25
FePt-25%C	20	25	30
FePt-30%C	25	30	35

Ar : 0.48 Pa
Deposition temperature: 600°C
Deposition rate: 0.15 nm/sec
Substrate : MgO(001)

B.S.D.Ch.S. Varaprasad et al. *IEEE Trans. Magn.* (2015) DOI: 10.1109/TMAG.2015.2435027.

FePt-30%C, *t*=10 nm

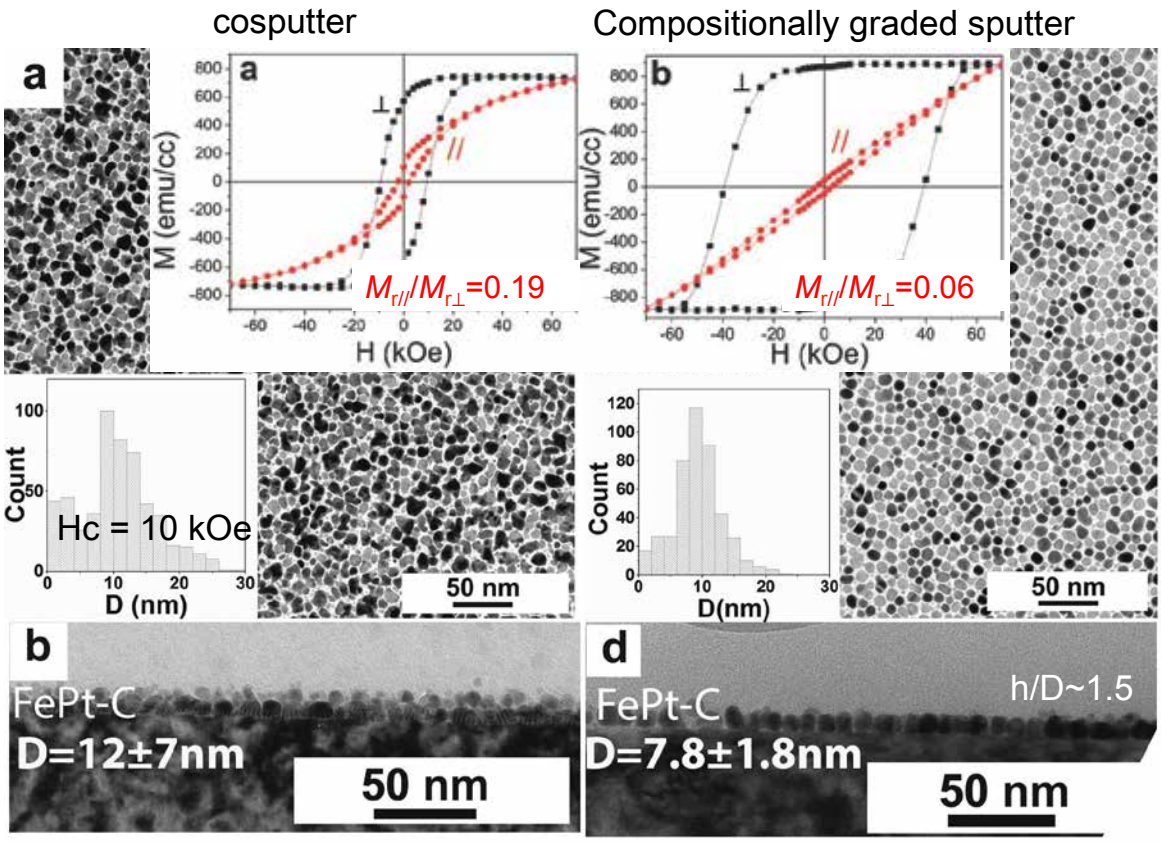

Microstructure

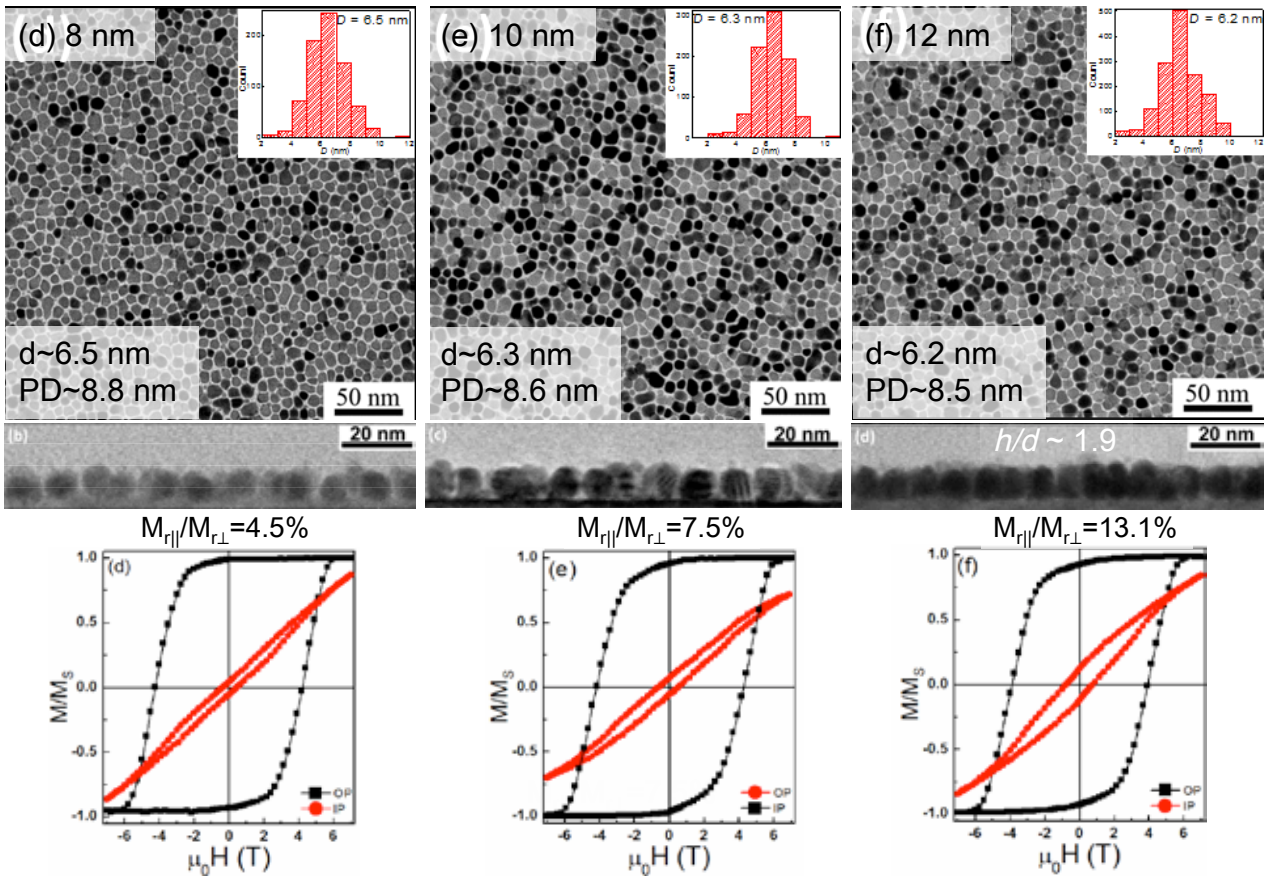

t_{FePt} layer : 12nm

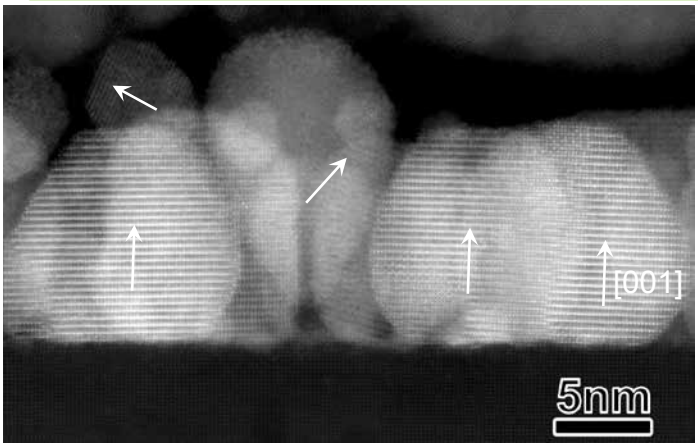

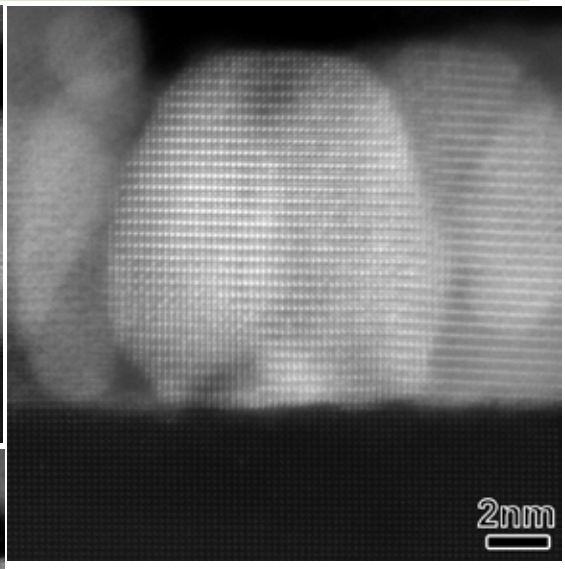

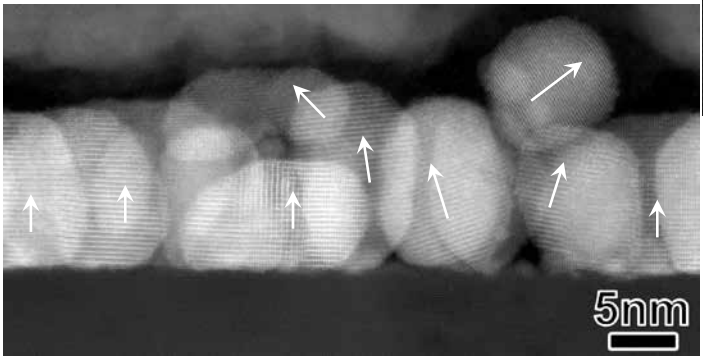

- The FePt grains with proper surface contact with MgO shows a good out of plate texture.

Read head for >2 Tbit/in²

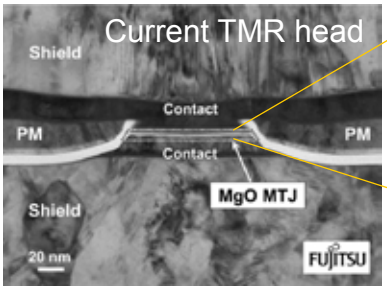

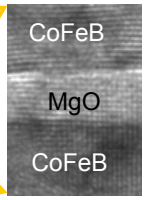

RA>1 Ωμm²

CoFeB/MgO/CoFeB

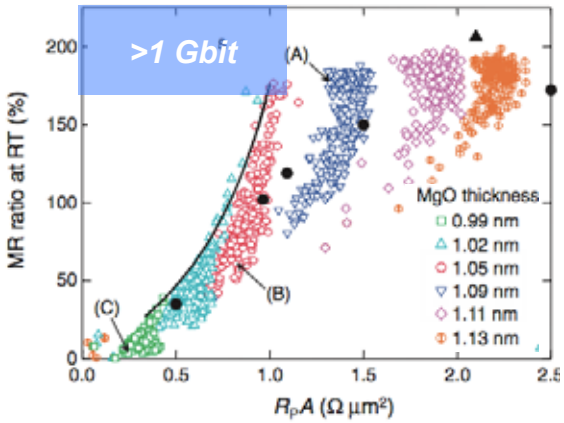

Hiroki Maehara et al, *Applied Physics Express* 4 (2011)

CPP-GMR

FM
NM
FM

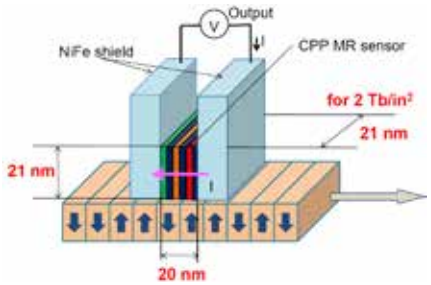

MR at low RA

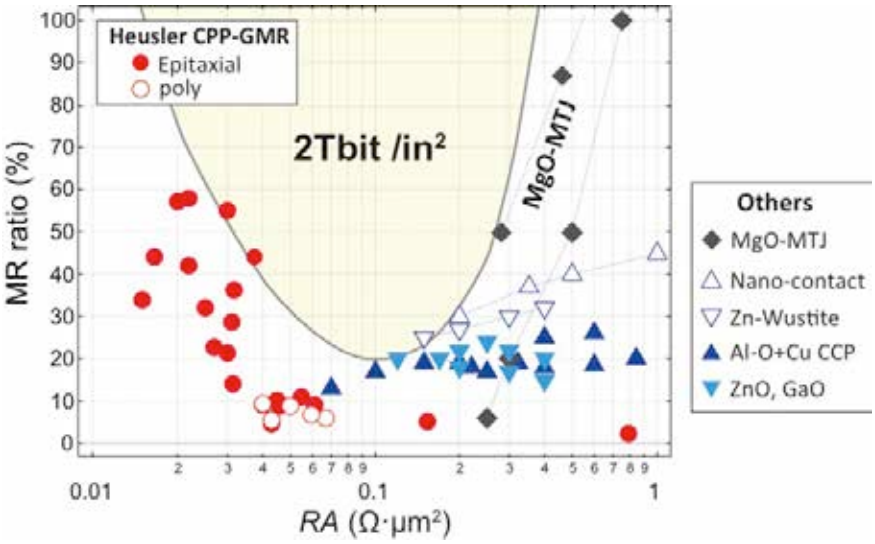

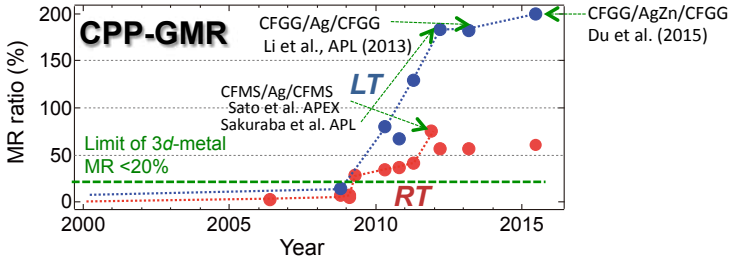

Takagishi et al. IEEE Trans. Magn. 46, 2086 (2010).

Magnetoresistive devices

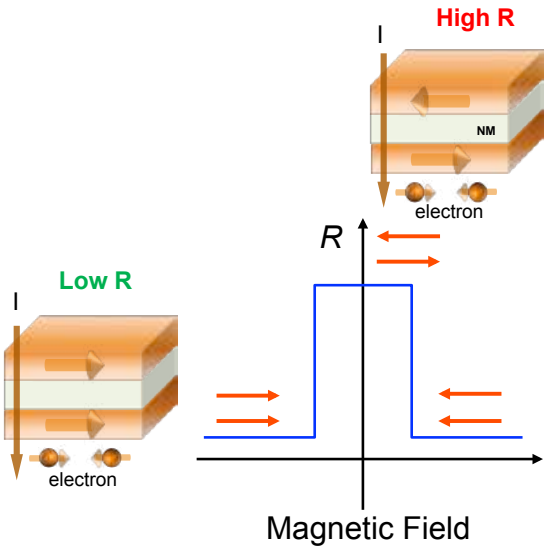

Tunneling Magnetoresistance

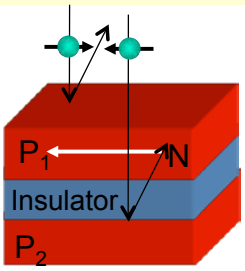

$$TMR = \frac{2P_1P_2}{1-P_1P_2}$$

Giant Magnetoresistance

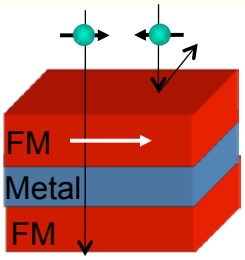

$$\Delta RA = \frac{4(\beta_P \rho_P^* t_P + \gamma AR^*)^2}{\rho_P^* t_P + \rho_F^* t_F + \rho_N t_N + 2AR^* + R_{para}}$$

Coherent tunneling

epitaxial Fe (001)/MgO(001)/Fe(001) structure

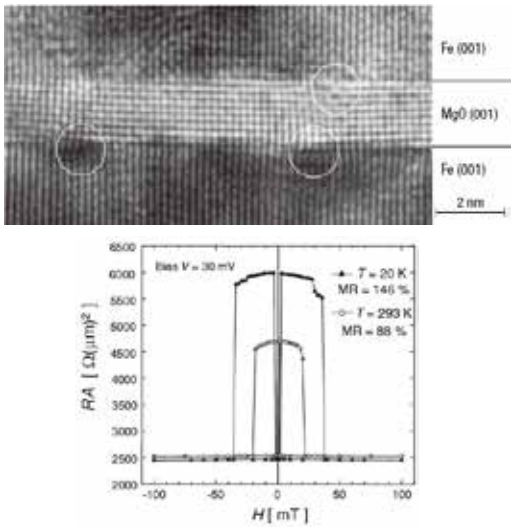

S. Yuasa *et al.* Nature Materials, **3**, 868 (2004)

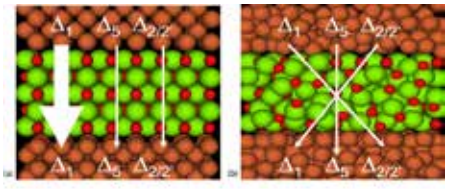

A V Khvalkovskiy et al. J. Phys. D, 46 074001 (2013)

Energy band dispersion of Fe [001]

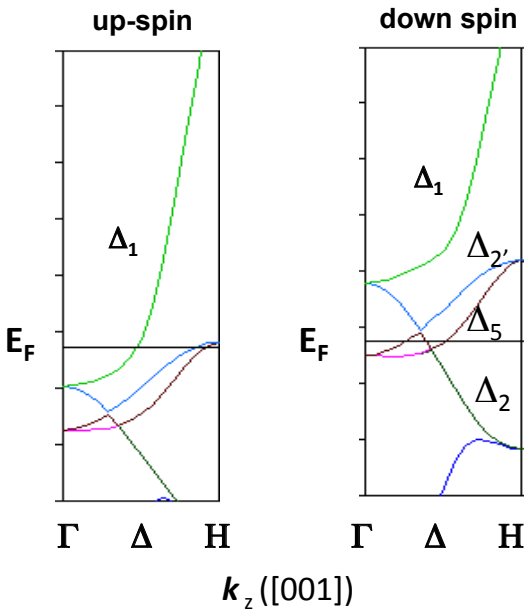

S. Yuasa et al. JJAP, 43, L588 (2004)

Spin polarization of conductive electron

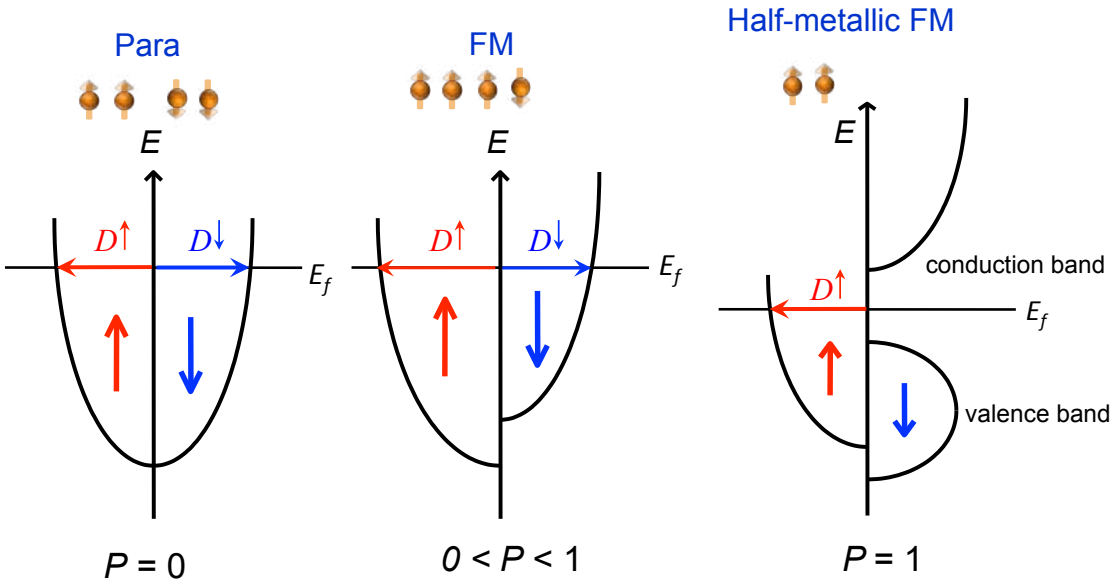

$$P = \frac{D\uparrow(E_f) - D\downarrow(E_f)}{D\uparrow(E_f) + D\downarrow(E_f)}$$

P : spin polarization

CPP-GMR and FM Heusler alloys

$$\Delta RA \approx 2\rho_F \frac{\beta^2}{1-\beta^2} t_F + 4AR_{F/N} \frac{\gamma^2}{1-\gamma^2}$$

bulk interface

For 1 Tb/in²
MR ~ 10-20%
ΔV =ΔRA x J= MR% x V_{BIAS}>12 mV
12% MR & J ~ 2x10⁸ A/cm²
after Jeff Childress, HGST

Co_2FeZ or Co_2MnZ Heusler alloys

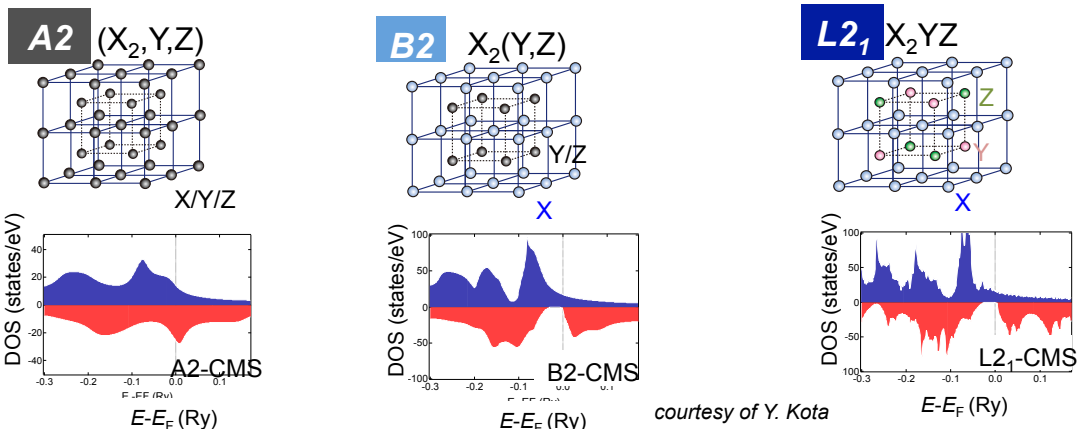

Search for highly spinpolarized FM alloys

DOS calculation

DOS calculations: VASP

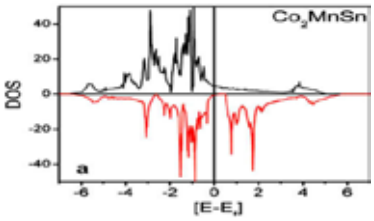

Alloy preparation

arc melting or induction meting

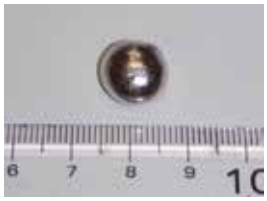

+ annealing

XRD & Thermal analysis

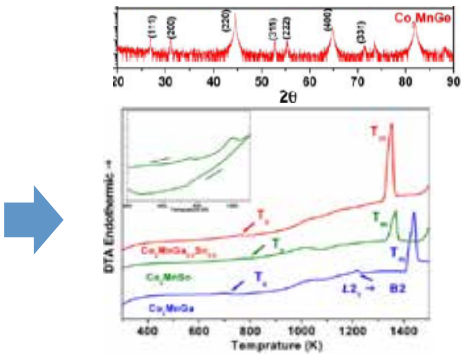

Tc, order-disorder temperature, melting point

Spin polarization

Point Contact Andreev Reflection (PCAR)

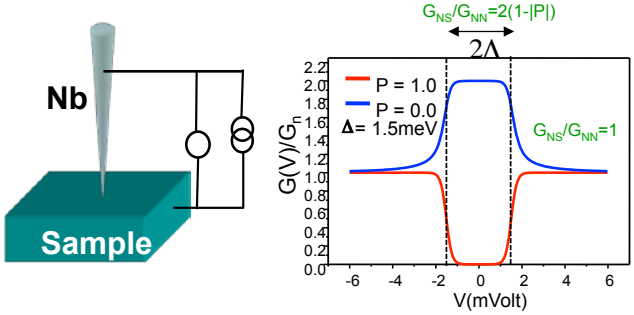

Conductance–bias

Spin polarization measured by PCAR

Quaternary alloys	P(%)	Ref.
$Co_2Mn(Ge_{0.75}Ga_{0.25})$	74	1
$Co_2Mn(Ga_{0.5}Sn_{0.5})$	72	2
$Co_2Fe(Si_{0.75}Ge_{0.25})$	70	3
$Co_2Fe(Ga_{0.5}Ge_{0.5})$	68	4
$Co_2(Cr_{0.02}Fe_{0.98})Ga$	67	5
$Co_2Mn(GeSn)$	67	6
$Co_2(Mn_{0.95}Fe_{0.05})Sn$	65	7
$(Co, Fe)_2MnGe$	65	8
$Co_2(Mn_{0.5}Fe_{0.5})Ga$	65	9
$Co_2(Cr_{0.02}Fe_{0.98})Si$	65	10
$Co_2Mn(Ti,Sn)$	64	11
$Co_2Mn(Al_{0.5}Sn_{0.5})$	63	12
$Co_2Mn(Ga_xSi_{1-x})$	63	13
$Co_2Fe(Al.Ga)$	63	14
$Co_2Mn(SiGe)$	63	15
$Co_2(Mn_{0.5}Fe_{0.5})Si$	61	16
$Co_2(Cr,Fe)Al$	60	17
$Co_2Mn(Al_{0.5}Si_{0.5})$	60	18
$Co_2Fe(Ga_{0.5}Si_{0.5})$	60	19
$Co_2Fe(Al_{0.5}Si_{0.5})$	60	20

Ternary alloys	P	Ref.
Co_2MnSi	56	21
Co_2MnGe	58	1
Co_2MnSn	60	12
Co_2MnAl	60	12
Co_2MnGa	60	1
Co_2CrAl	62	17
Co_2FeAl	59	17
Co_2FeSi	60	10
Co_2FeGa	58	22
Co_2CrGa	61	23
Co_2TiSn	57	24
Co_2VAl	48	25
Fe_2VAl	56	25

Metals and binary	P	Ref.
Fe	46	
Co	45	
FeCo	50	
$Co_{75}Fe_{25}$	58	
B2-FeCo	60	
$[Co/Pd]_n$	60	
Fe_4N	59	26
Co/Pt	56	27

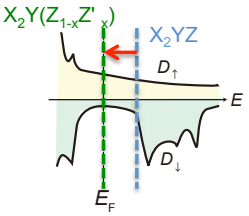

1. B. Varaprasad *et al.*, APEX**3** 023002 (2010).
2. B. Varaprasad *et al.*, Acta Matel.**57** 2702 (2009).
7. A. Rajanikanth *et al.*, JAP**103** 103904 (2008).
10. S.V. Karthik *et al.*, JAP**102** 043903 (2007).
12. A. Rajanikanth *et al.*, JAP**101** 09J508 (2007).
17. S.V. Karthik *et al.*, APL**89** 052505 (2006).
20. T.M. Nakatani *et al.*, JAP**102** 033916 (2007).
21. A. Rajanikanth *etal.*, JAP**105** 063916 (2009).
23. T.M. Nakatani *et al.*, JPD**41** 225002 (2008).
25. S.V. Karthik *et al.*, Acta Matel.**55** 3867 (2007).
26. A. Narahara *et al.*, APL**94** 202502 (2009).
27. A. Rajanikanth *et al.*, APL**97** 022505 (2010).
3-6, 8,9,11,13-17,18-20,22,24. To be submitted

V. Varaprasad et al. Acta Mater (2012).

ΔRA increase by annealing

$Co_2Fe(Ga_{0.5}Ge_{0.5})$ B.S.D.Ch.S. Varaprasad et a. Acta Mater. 60, 6257 (2012).

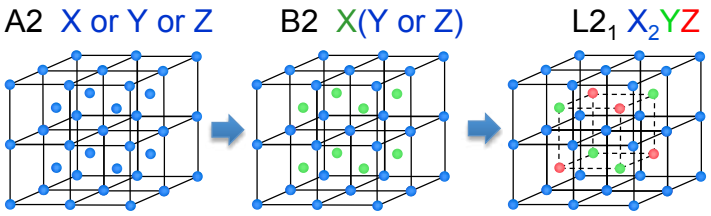

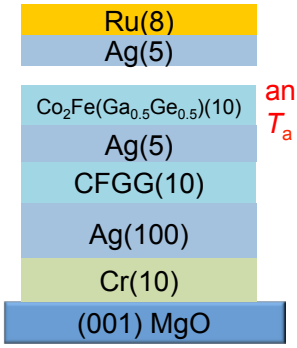

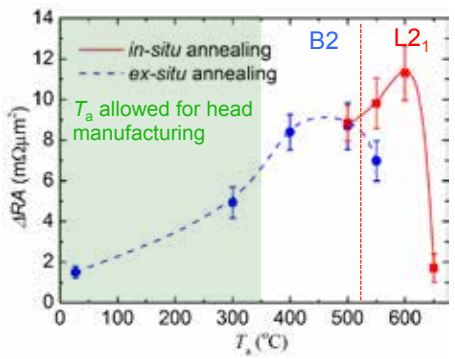

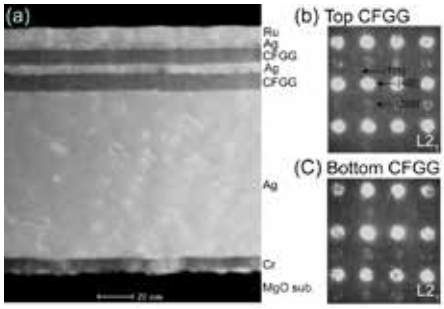

S. Li, Y.K. Takahashi, T. Furubayashi, and K. Hono, APL 103, 042405 (2013).

Large temperature dependence of MR

ΔRA= 12 mΩμm², ΔR/R=57%

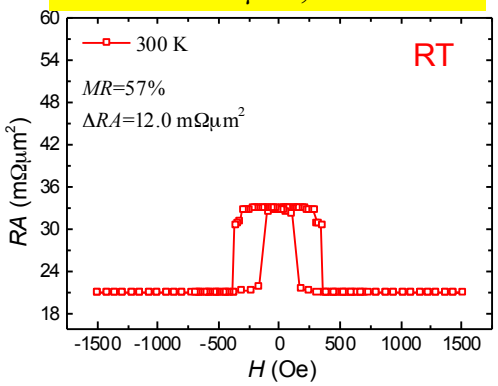

ΔRA= 33 mΩμm², ΔR/R=183%

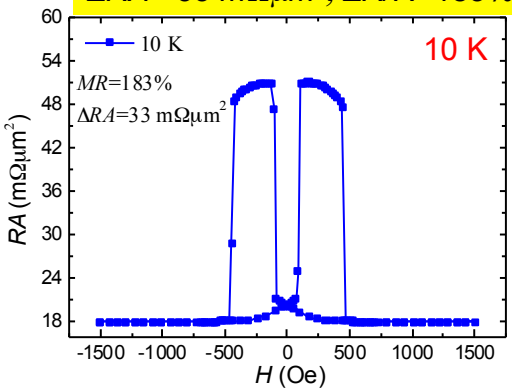

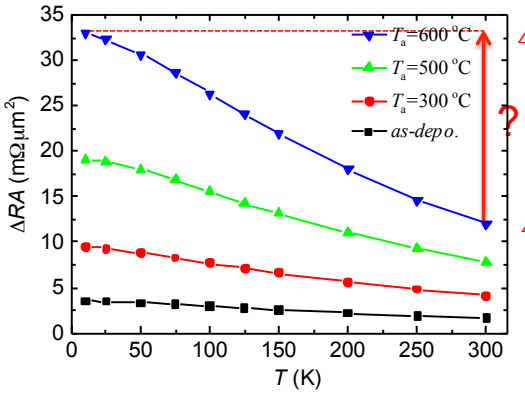

ΔR/R=183%

?

ΔR/R=57%

S. Li, Y.K. Takahashi, T. Furubayashi, and K. Hono, APL 103, 042405 (2013).

Origin of T dependence of *ΔRA*

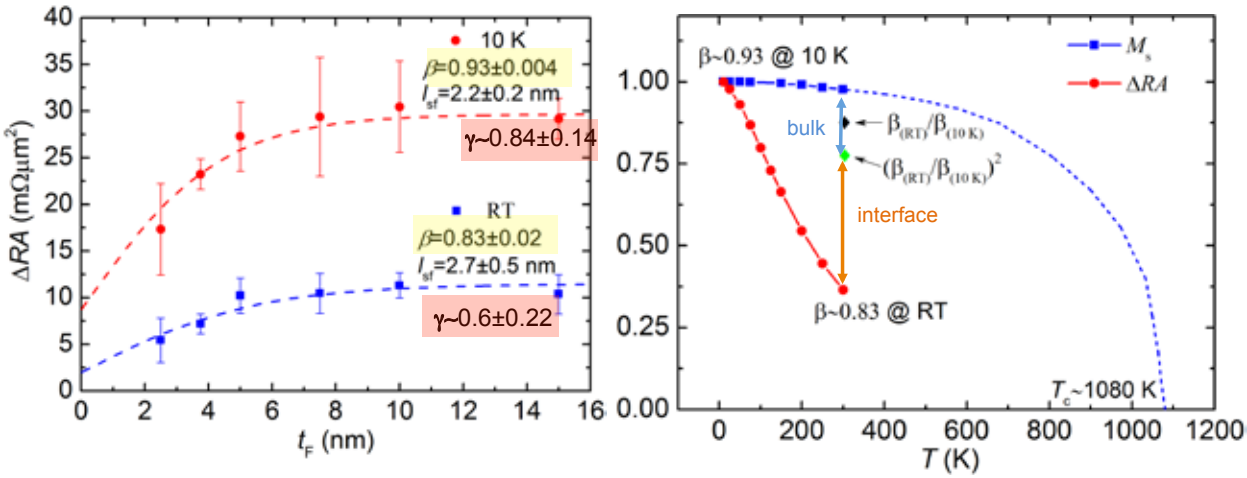

$$\Delta RA \approx 2\rho_F \frac{\beta^2}{1-\beta^2} t_F + 4AR_{F/N} \frac{\gamma^2}{1-\gamma^2}$$

Which contributes to T-dependence of *ΔRA*, β or γ?

Eveluation of β using AMR measurements

Anisotropy magnetoresistance (AMR)

$$\frac{\Delta\rho}{\rho} = \frac{\rho_{//} - \rho_{\perp}}{\rho_{//}} \times 100(\%)$$

$\rho_{//} > \rho_{\perp}$: Positive

$\rho_{//} < \rho_{\perp}$: Negative

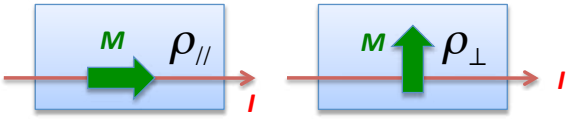

Ferromagnet

Theory of AMR and spin asymmetry by Kokado

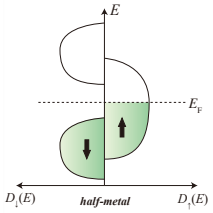

Half-metal: no $D_\downarrow(E_F)$ +, no $D_\uparrow(E_F)$ -

$$\frac{\Delta\rho}{\rho} \propto \gamma(D_\uparrow^{(d)} - D_\downarrow^{(d)})(\sigma_\downarrow - \sigma_\uparrow)$$

- + → AMR is always ***negative*** in half-metal

$$\frac{D_\downarrow}{D_\uparrow} \propto 1 + \frac{\Delta\rho/\rho}{c}$$

■$\Delta\rho/\rho < 0$, $|\Delta\rho/\rho|$↑ → $D_\downarrow/D_\uparrow$↓ → P↑.

Kokado et al. (J. Phys. Soc. Jpn. 81, 024705 (2012))

ΔRA and AMR

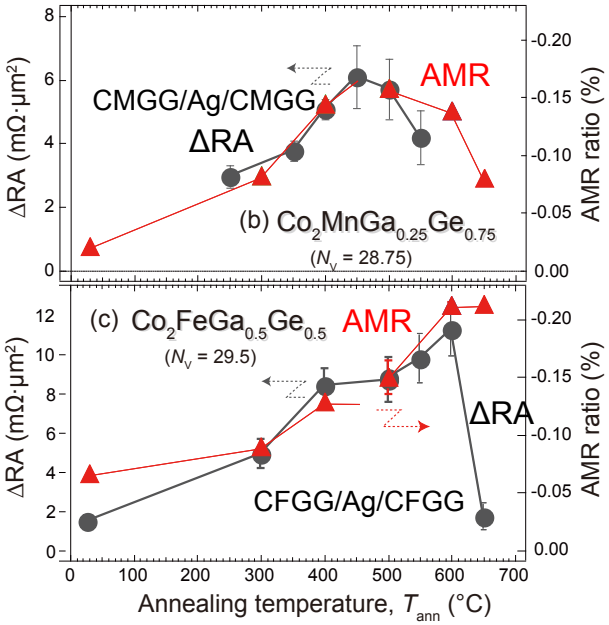

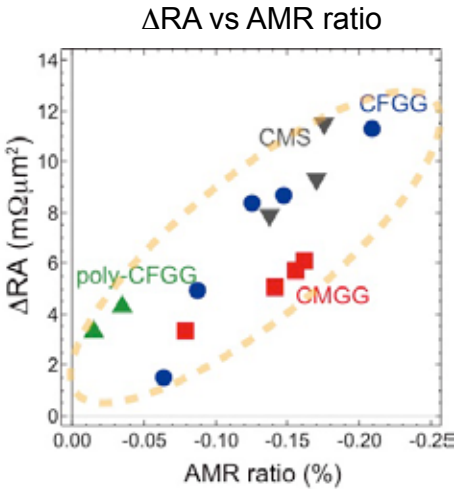

Excellent correlation between AMR and ΔRA

Facile way to estimate β

Y. Sakuraba et a. APL104, 172407 (2014).

Temperature dependence of Δρ

$\Delta\rho(T) = \mathrm{AMR}(T) \times \rho(T)$

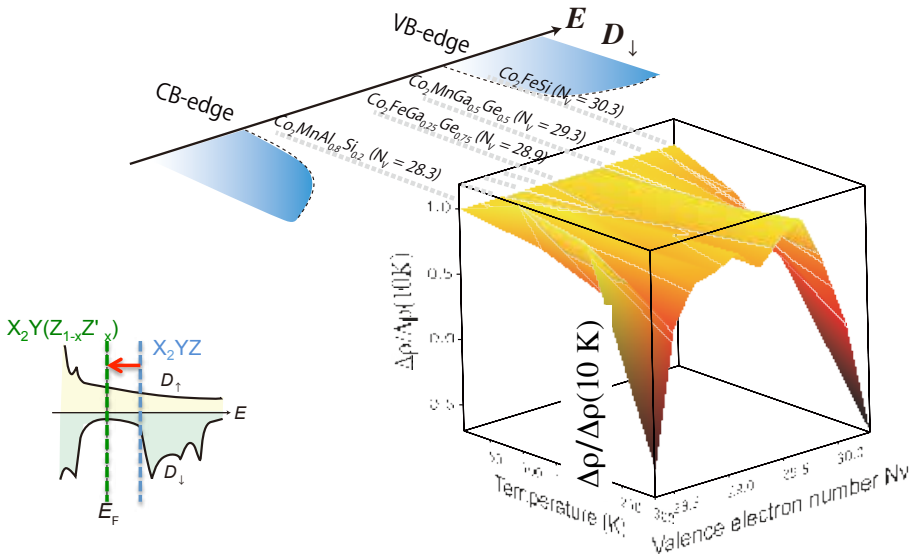

β of CFGG does not degrade at RT!

Y. Sakuraba et a. APL104, 172407 (2014).

Band matching at FM/NM interface

- Rh_2CuSn ($L2_1$)

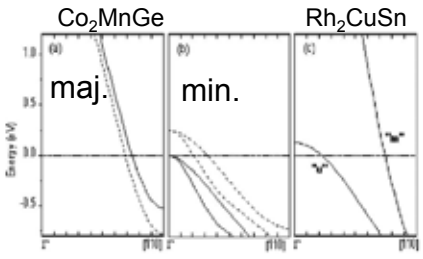

thickness dependence

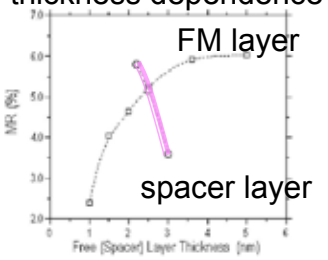

K. Nikolaev et al., Appl. Phys. Lett. 94, 222501(2009)

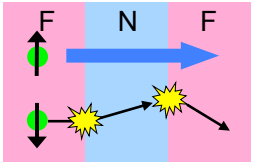

$\Delta RA \propto AR_{F/N} \cdot \gamma^2/(1-\gamma^2)$

small $R_{F/N}$ for up spin
large $R_{F/N}$ for down spin → small total $R_{F/N}$

All B2 CPP-GMR

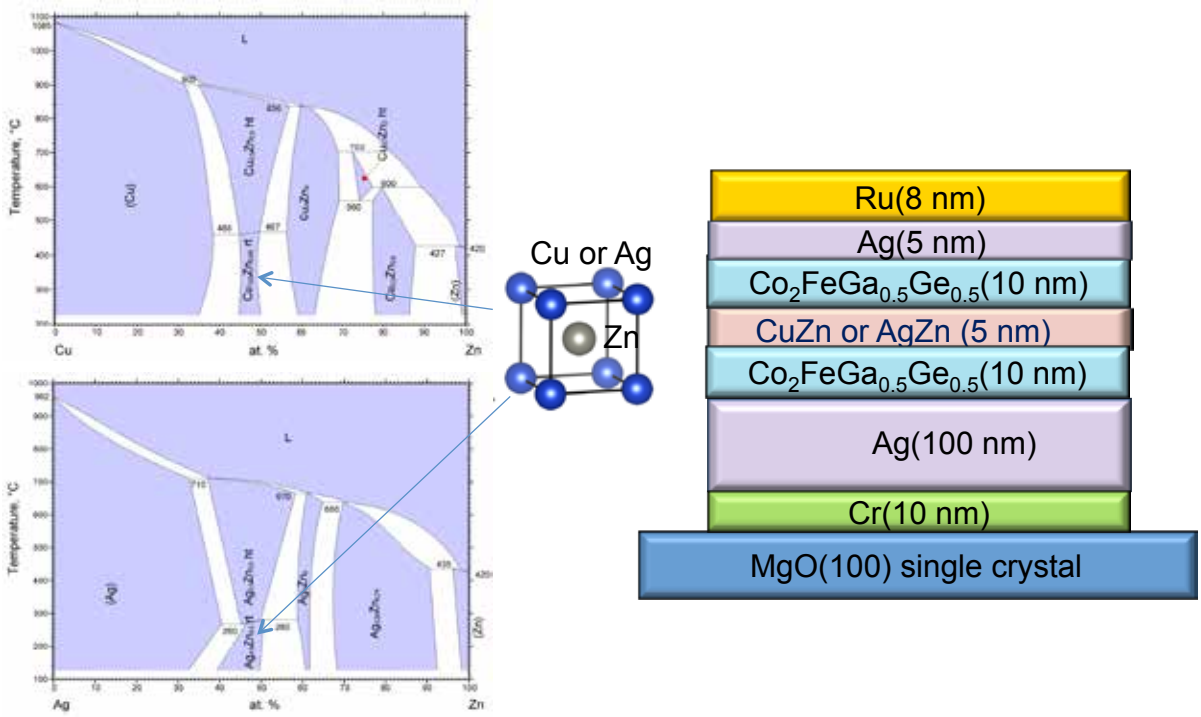

ΔRA and T_a of Heusler/NM/Heusler PSV

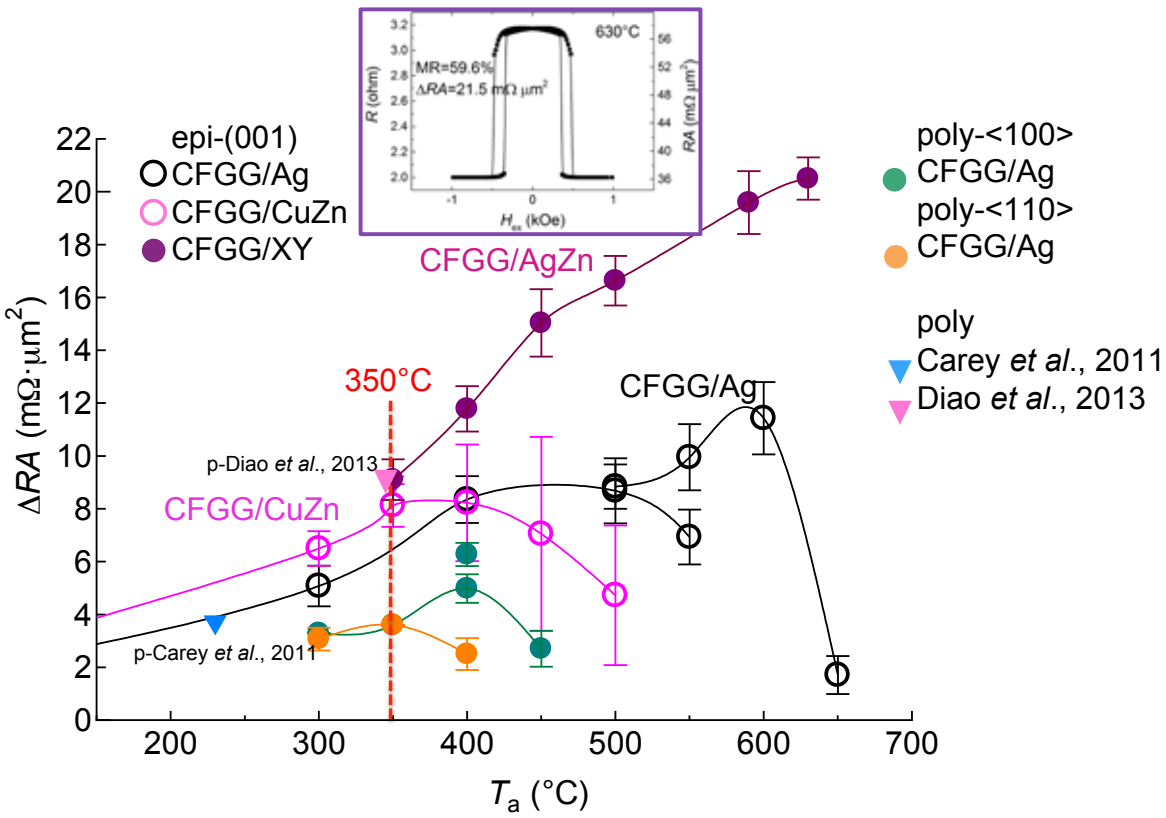

Y. Du et al. APL, 2015.

Interlayer diffusion during annealing

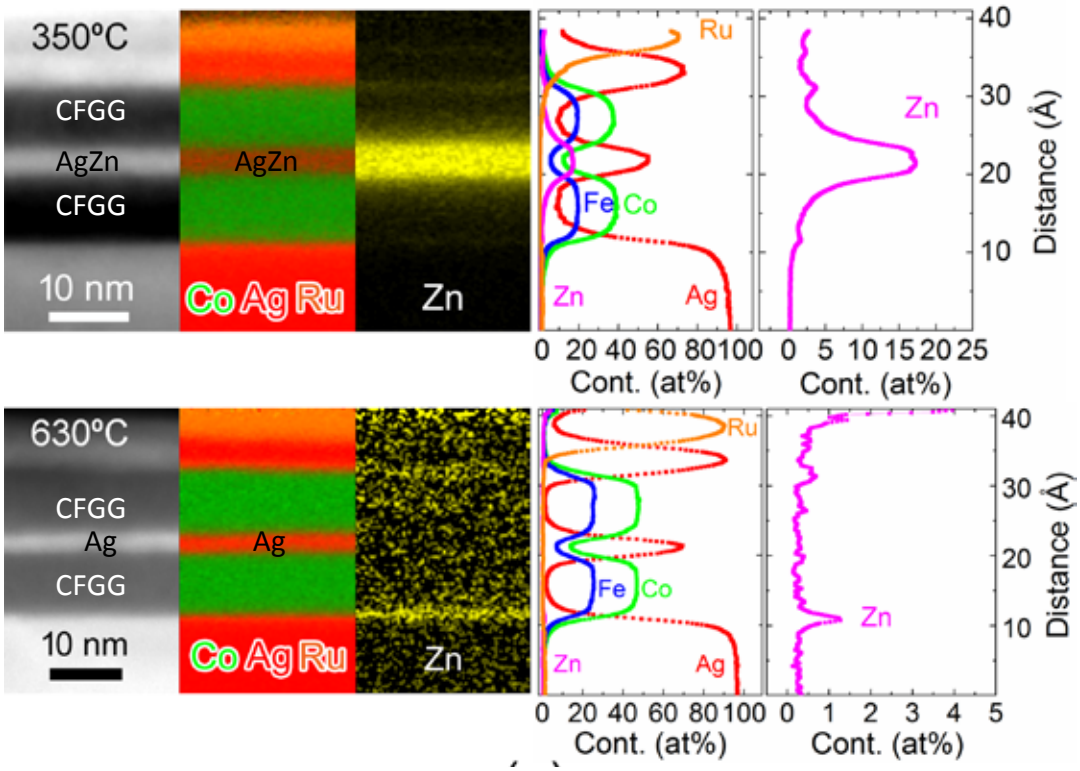

Structure change of AgZn spacer layer

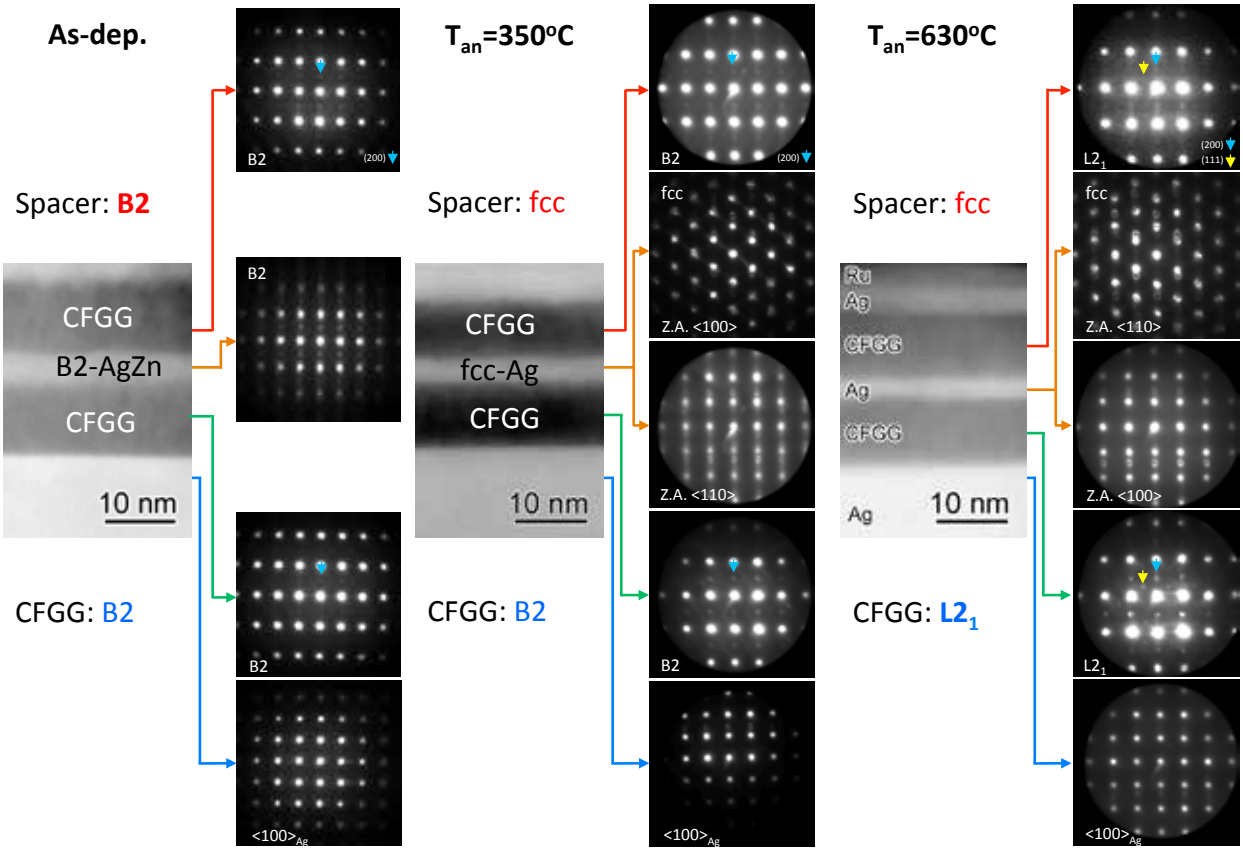

Improvement of γ by band matching

Why NiAl insertion ?

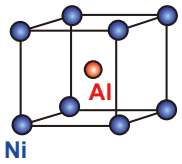

▪ ***B2 structure, a = 0.288 nm***
⇨ ***Good structural and band structure matching***

Calculated transmittance based first-principles calculation

CFGG/**NiAl(B2)**/CFGG

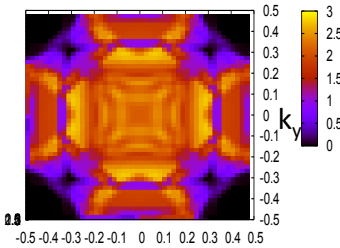

CFGG/**Ag(fcc)**/CFGG

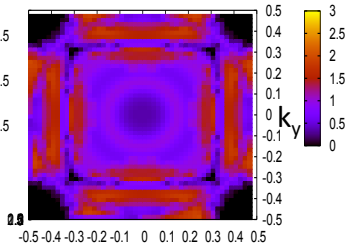

Calculated by Y. Miura

RA = 2.9 mΩμm² RA = 4.5 mΩμm²

Better band matching between CFGG and NiAl.

Disadvantage of NiAl

Short spin diffusion length of NiAl ~ 8 nm

cf. Ag > 200 nm

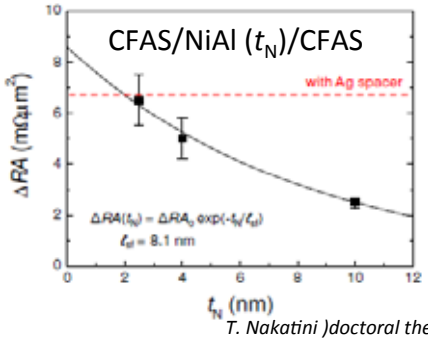

T. Nakatini)doctoral thesis)

Small ΔRA using thick NiAl spacer because of spin relaxation

This study

T_{ann} = 550°C

B2-NiAl (t_{NiAl} = 0.2-0.6 nm)

Improve band matching by inserting thin NiAl to Ag spacer interface ?

Large MR in CPP-GMR with NiAl insertion

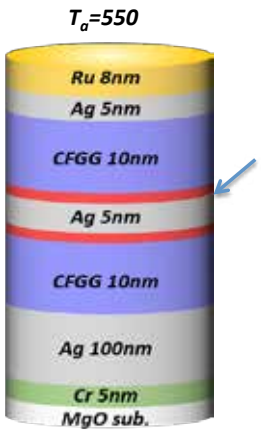

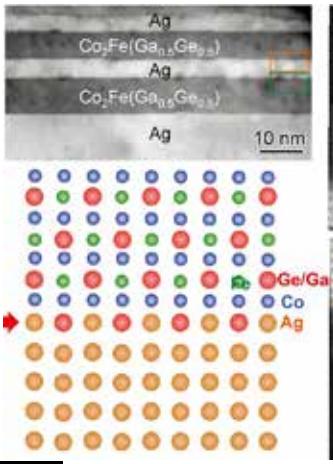

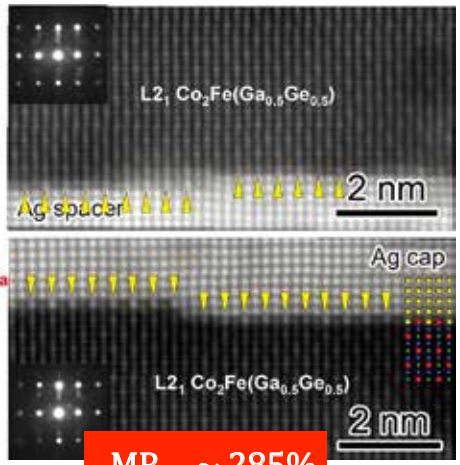

MR_{int} ~ 82% t_{NiAl} = 0.21 nm

ΔRA ~ 31mΩμm²

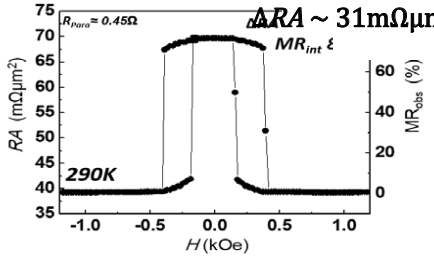

MR_{int} ~ 285% t_{NiAl} = 0.21 nm

ΔRA ~ 78mΩμm²

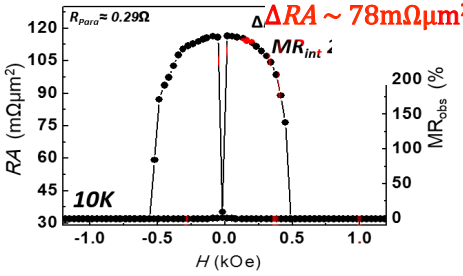

MR-RA updated benchmark

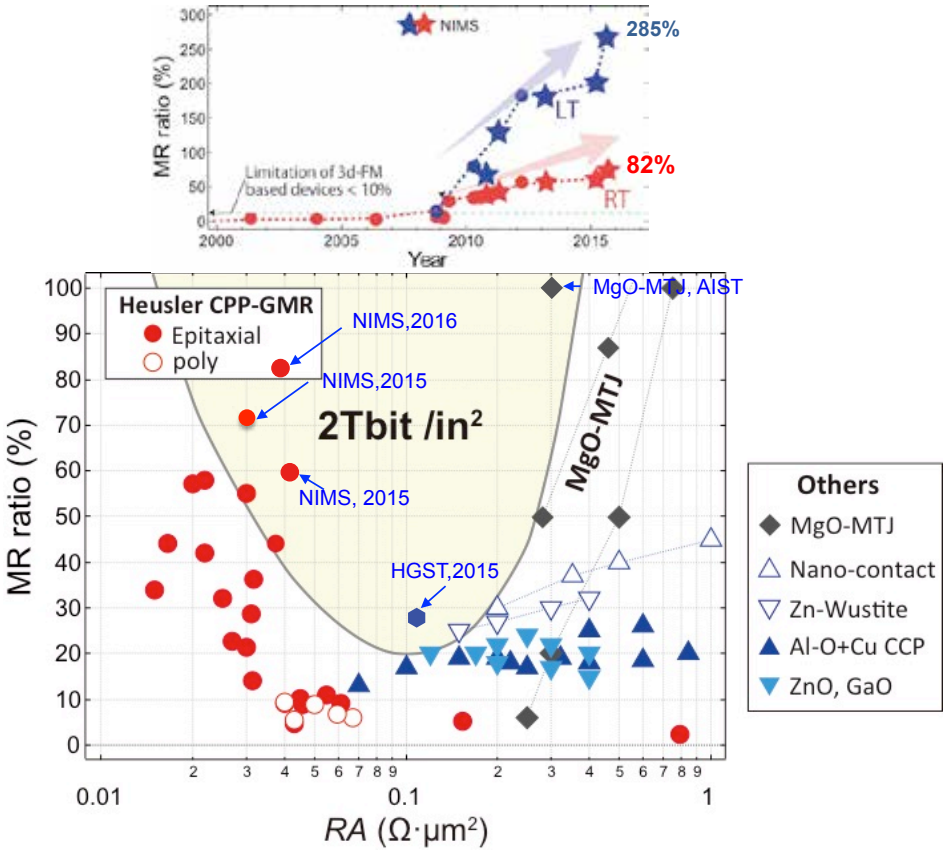

Summary

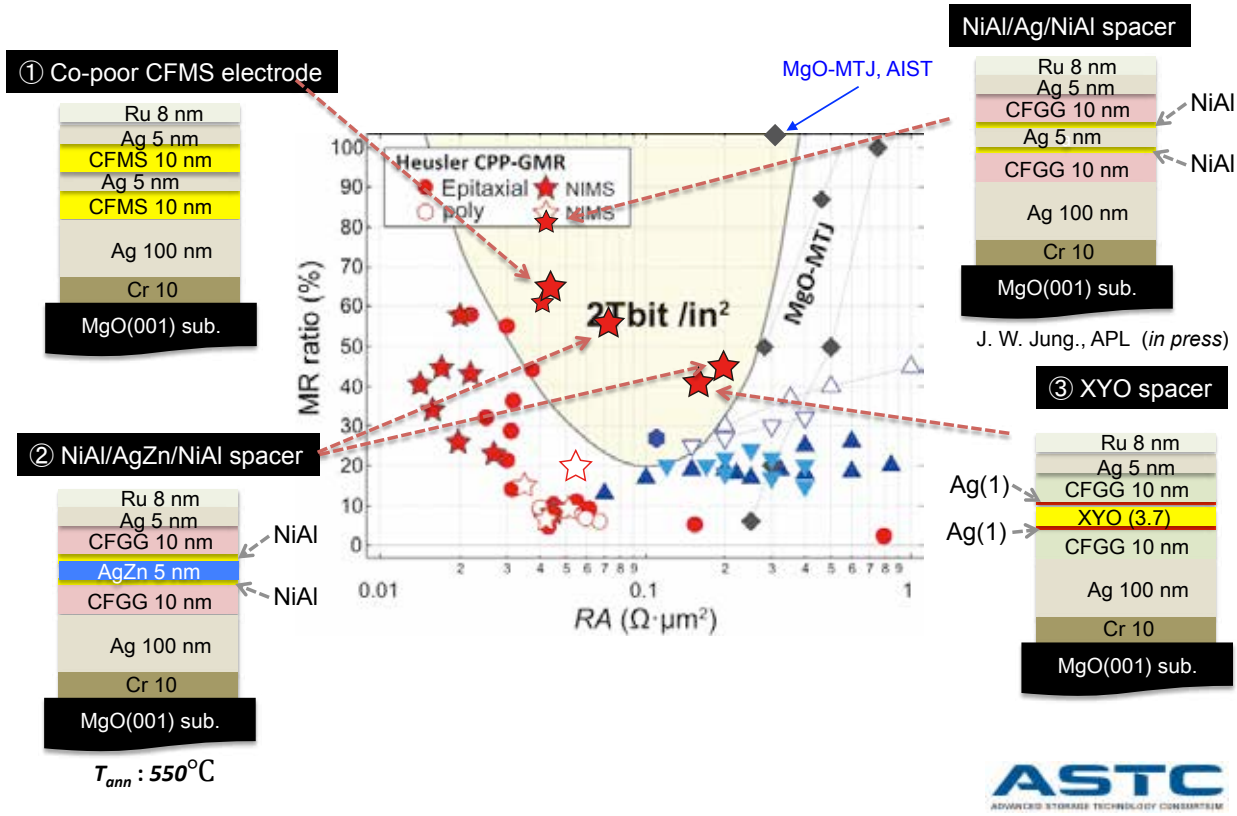

Epi. VS Poly.

CFGG stands for $Co_2FeGa_{0.5}Ge_{0.5}$

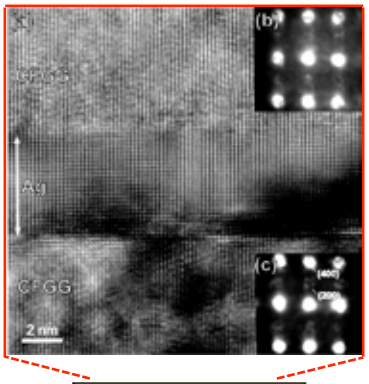

MR ratio=41.7% at RT
RA=9.5

VS

MR ratio=~10% at RT
RA=~4

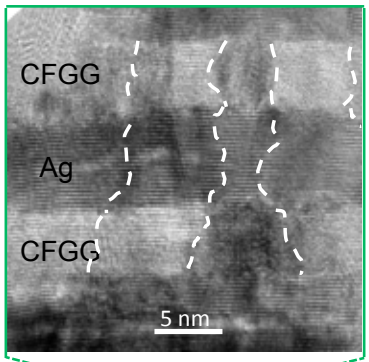

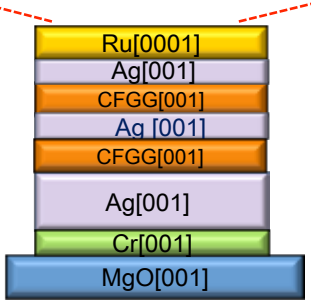

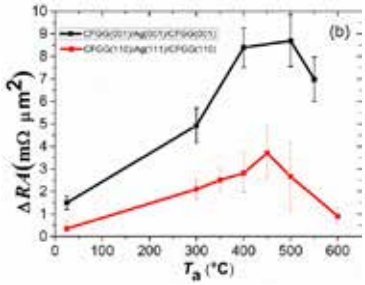

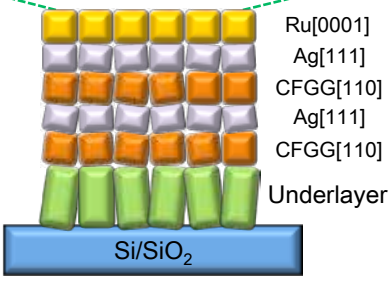

(100)-oriented Epitaxial Film structure

(110)-oriented Polycrystalline Film structure

$(001)_{CFGG}/(001)_{Ag}$ interface >> $(011)_{CFGG}/(111)_{Ag}$ interface

0.7%
0.7%
<<
0.7%
18.9%

Polycrystalline CFAS PSV on Si substrate

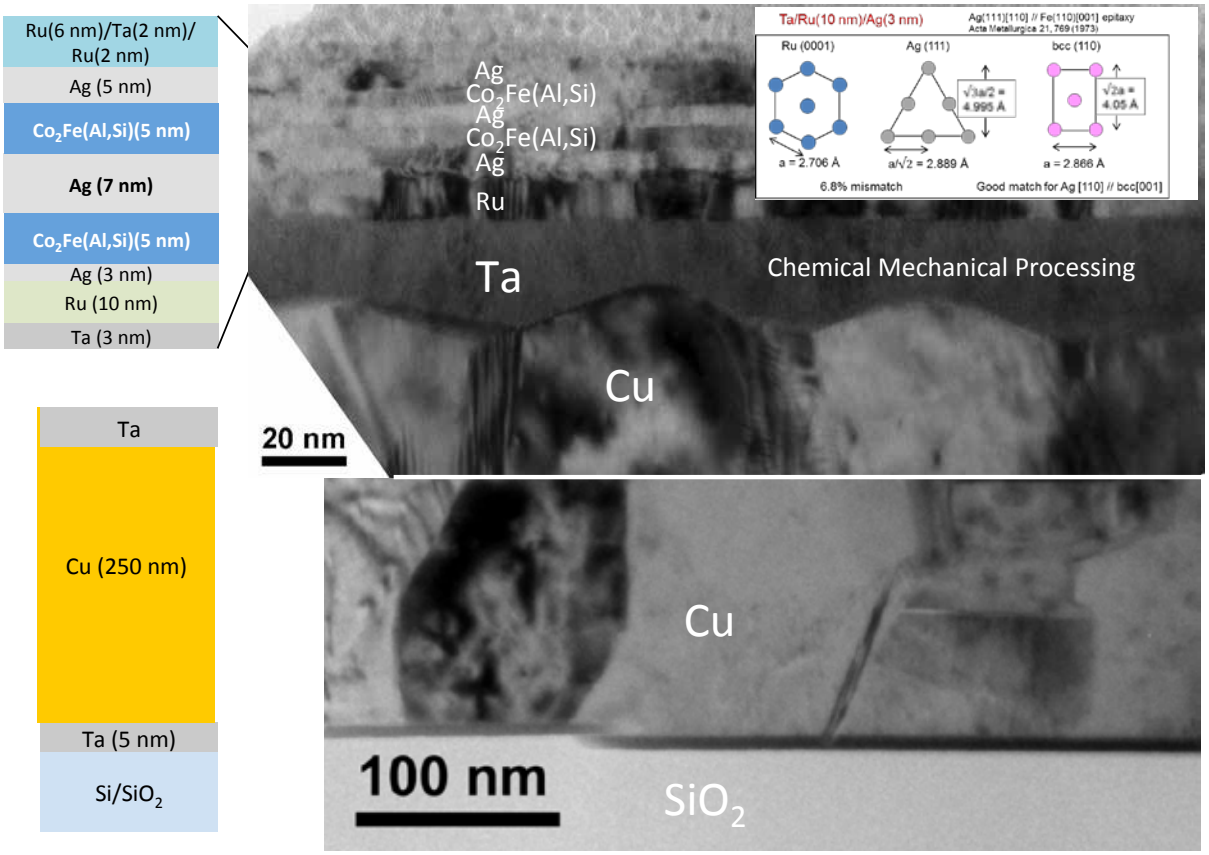

In-plane TEM observations of CFAS layer

SiO2//Ta/Ru/Ag/CFAS(20 nm)/Ag(10 nm)

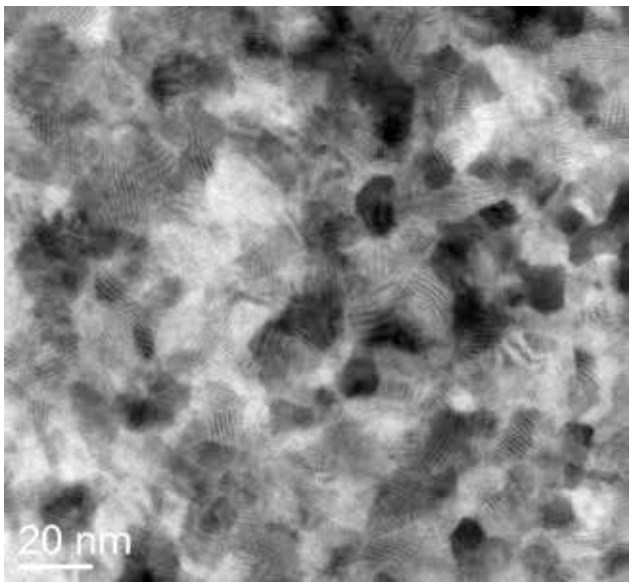

CFAS 400 C

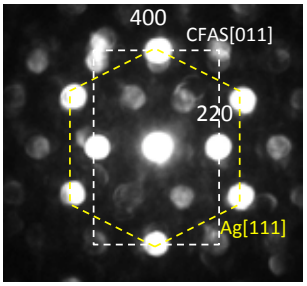

CFAS 450 C

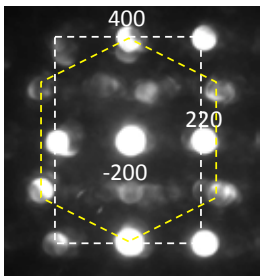

CFGG 350 C

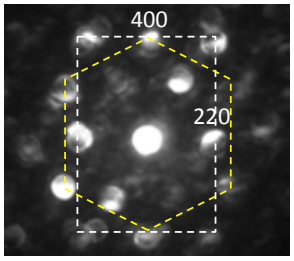

OR: $[111](220)_{Ag}$ //$[011](002)_{Heusler}$

T.M. Nakatani, Ye Du, Y.K. Takahashia, T. Furubayashi, K. Hono, Acta Mater. 61, 3695 (2013).

Two approaches toward low RA & high MR devices

MR>300%, RA<0.8Ωμm²
for 10X STT-MRAM and spin-logic

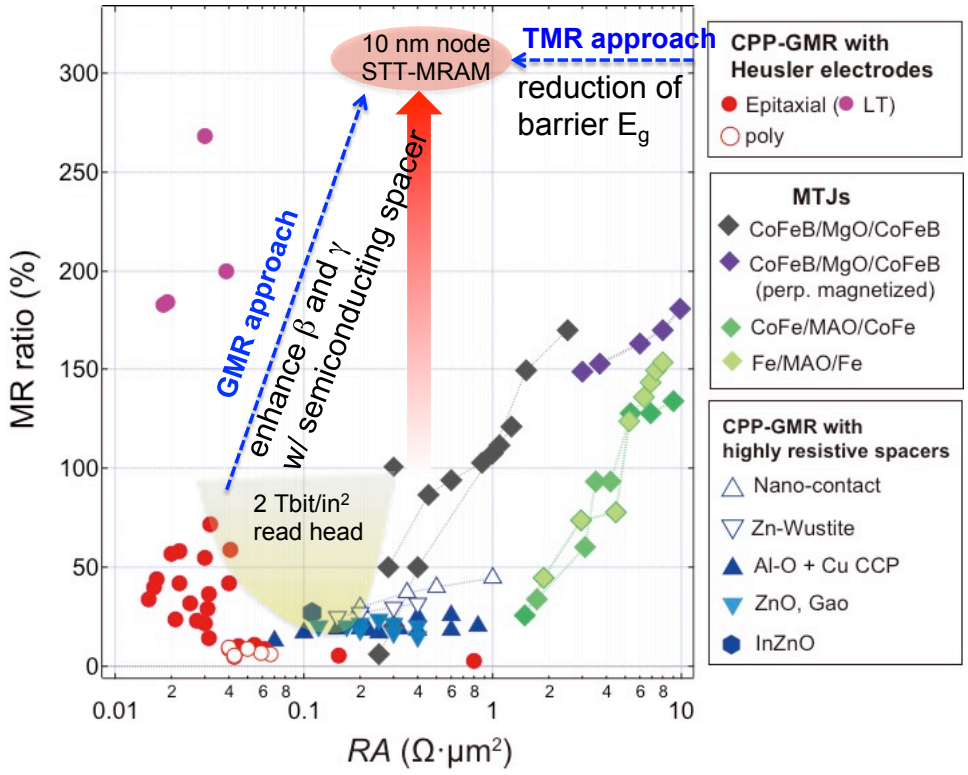

Prospect of CPP-GMR sensors

RA ~ 30-60 mΩμm², MR = 40-60%@RT

	HDD read sensor	MR for STT-RAM	Magnetic Sensor (earth magnet, automotive, bio)
Required	RA ~ 50 – 100 mΩμm² Polycrystalline device on pearmalloy T_{ann} < 350°C, high damping α	RA~100-500 mΩμm², MR ~ 300% high K_u, low M_s, low α, PMA	MR > 100%, linear response
Our approach	RT half-metal [001]-textured polycrystal New spacer (band matchin, large $R_{F/N}$), ΔRA > 15mΩμm²	Ferrimagnetic Heusler alloy low Eg, coherent tunneling	Multilayer、dual-spin valve Interlayer exchange coupling
Research subjects	New Heusler alloy New spacer material Understanding transport properties (VF, AMR, XMCD,theoretical), Growth on pearmalloy	Oxide spacer high MR using interface control Single crystalline device on Si	Interlayer exchange coupling

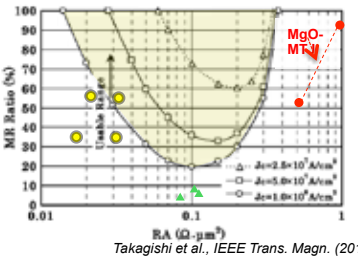

Takagishi et al., IEEE Trans. Magn. (2010).

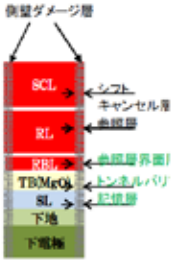

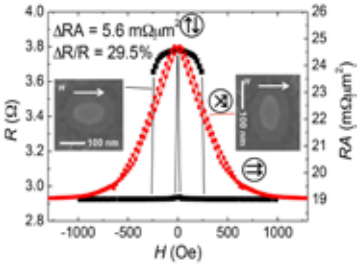

Acknowledgement


Y. Sakuraba


Y. K. Takahashi


T. Furubayashi


T. Nakatani


S. T. Li


S. Bosu

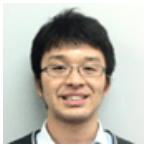
T. T. Sasaki


J. W. Jung

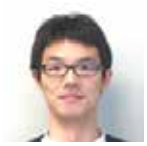
Ye Du


J. Chen

Magnetic Materials Unit

- **IEEE Magnetics Society Home Page:** ***www.ieeemagnetics.org***
  - 3000 full members
  - 300 student members
- **The Society**
  - Conference organization (INTERMAG, MMM, TMRC, etc.)
  - Student support for conferences
  - Graduate Student Summer Schools
  - Local chapter activities
  - Distinguished lectures
- **Journals (Free Electronic Access for Mambers)**
  - *IEEE Transactions on Magnetics*
  - *IEEE Magnetics Letters*
- **Online applications for IEEE membership:** ***www.ieee.org/join***
  - 360,000 members
  - IEEE student membership IEEE full membership

T dependence of μ_{Co} at CMS & CFS/Ag interfaces

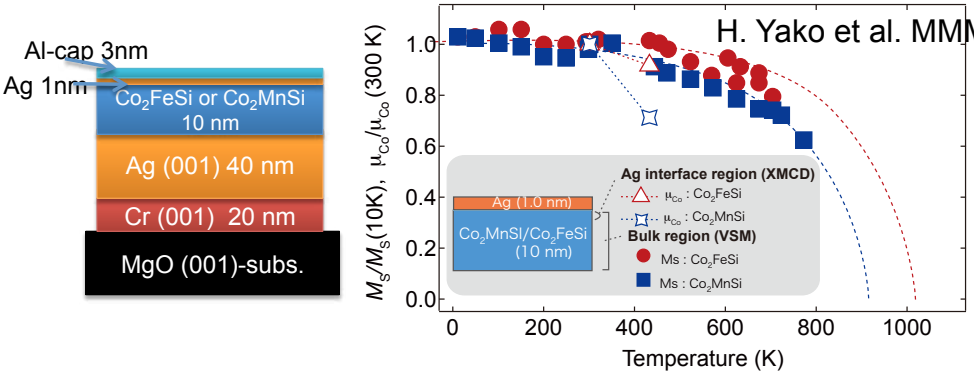

Ag(40) / Co_2MnSi (10) / Ag (1)

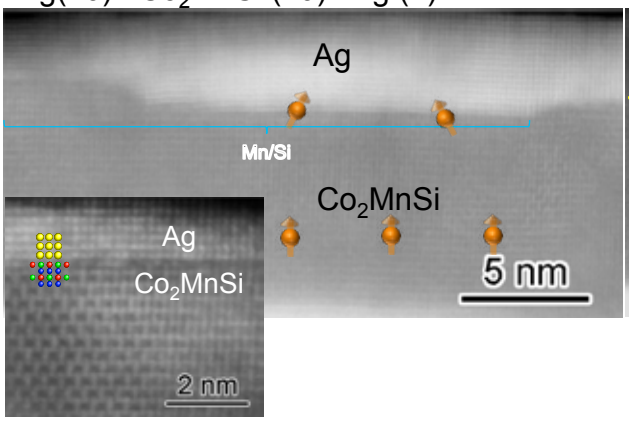

Ag(40) / Co_2FeSi (10) / Ag (1)

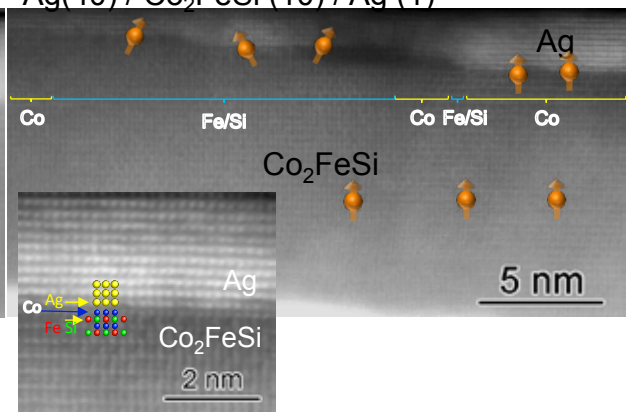

How to surpress the reduction of spin moment at Hesuer/Ag interface?

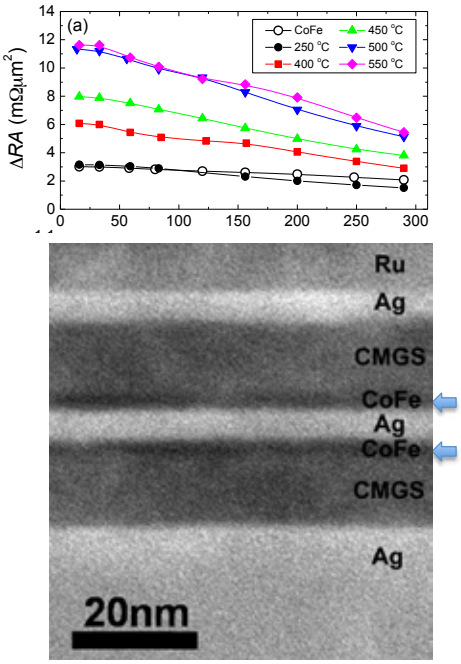

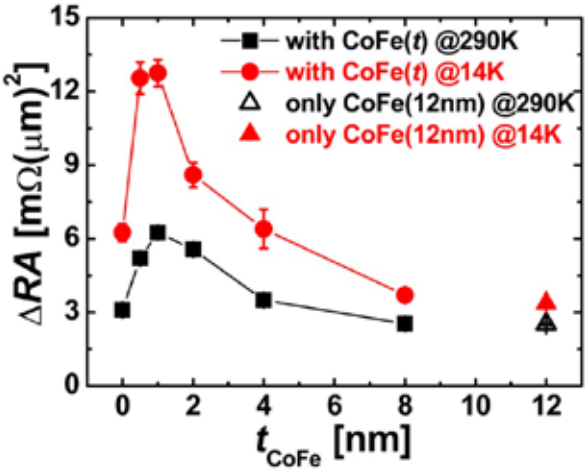

Insersion of thin FM layer for increasing exchange stiffness

N. Hase et al. JAP 109, 07E112 (2011).